

# CLIPA7 Exhibits Pleiotropic Roles in the *Anopheles gambiae* Immune Response

Renée Zakhia Mike A. Osta

Department of Biology, American University of Beirut, Beirut, Lebanon

## Keywords

*Anopheles gambiae* · Mosquito innate immunity · Clip domain serine proteases · Melanization

## Abstract

Clip domain serine proteases and clip domain serine protease homologs (cSPHs) are key components of serine protease cascades that drive the melanization response. Despite lacking catalytic activity, cSPHs play essential roles in regulating melanization, but the spectrum of functions they catalyze within and outside these cascades is not fully understood. Aside from their classical role as cofactors for PPO activation, we have previously revealed an unprecedented complexity in the function and molecular organization of these cSPHs in the immune response of the malaria vector *Anopheles gambiae*. Here, we add yet another dimension to the complex roles underpinning the contributions of cSPHs to mosquito immunity by showing that CLIPA7, a member of the expanded cSPH family, defines a novel branch within the cSPH network that is essential for the melanization of *Escherichia coli* but not *Plasmodium* ookinetes or Gram-positive bacteria. Despite its dispensability for the melanization of Gram-positive bacteria, we show that CLIPA7 is required for the clearance of systemic infections with *Staphylococcus aureus*. CLIPA7 is produced by hemocytes and associates with the surfaces of live *E. coli* and *S. aureus* cells in vivo as well as with those of melanized cells. Based on its RNAi phenotypes

and its unique domain architecture among *A. gambiae* cSPHs including the presence of an RGD motif, we propose that CLIPA7 exhibits pleiotropic roles in mosquito immunity that extend beyond the regulation of melanization to microbial clearance.

© 2022 The Author(s).

Published by S. Karger AG, Basel

## Introduction

Clip domain serine proteases (cSPs) are the main components of serine protease cascades that regulate key insect immune responses including antimicrobial peptide synthesis in the Toll pathway and melanization (reviewed in [1–4]). cSPs are secreted into the insect hemolymph as zymogens and are composed of 1–5 clip domains at the N-terminus and a protease domain at the C-terminus [2, 5, 6]. In response to infection, cSPs are cleaved at a specific site in the N-terminus of the protease domain; however, the clip and the protease domains remain associated by a disulfide bond. Analysis of insect genomes identified a good number of cSPs containing protease-like domains [5–9], which are predicted to lack catalytic activity due to replacements in one or more of the amino acid residues (His, Asp, Ser) that form the catalytic triad [10–13], and are referred to as cSP homologs (cSPHs). Despite being noncatalytic, cSPHs require cleavage at a specific site within the clip domain to become functional [10, 13–16],

although several are predicted to have cleavage sites in the N-terminus of the protease-like domain [5]. Phylogenetic analysis of cSPs in the major African vector of malaria *Anopheles gambiae* classified them into five subfamilies; groups B, C, and D are mainly cSPs, group A includes only cSPHs, while group E genes are either cSPHs or hybrids containing both catalytic and noncatalytic domains [5].

Clip cascades have been characterized at the biochemical and genetic levels in the context of melanization and Toll activation in few insect species. They are activated by an upstream nonclip, modular serine protease (ModSp) that interacts with pattern recognition receptors bound to their cognate ligands and undergoes autocatalytic activation [17–21]. In general, active ModSp cleaves a CLIPC which in turn cleaves a prophenoloxidase-activating protease (PAP) of the CLIPB family. PAPs cleave prophenoloxidase (PPO) zymogen into active phenoloxidase which initiates the process of melanin biosynthesis on microbial surfaces (reviewed in [2, 3]).

While the roles of ModSp and cSPs in the context of these cascades are fairly well characterized, how cSPHs exert their functions is not fully defined. Biochemical studies in *Manduca sexta* [13, 16, 22, 23], *Tenebrio molitor* [15, 24], *Holotrichia diomphalia* [14], and *Helicoverpa armigera* [25] revealed that cSPHs act as cofactors for the efficient activation cleavage of PPO by a PAP of the CLIPB family. PPOs cleaved by their specific PAPs did not show any activity in vitro in the absence of their respective cSPH cofactors, suggesting that cSPHs are required for the proper cleavage of PPO [24, 26, 27]. Subsequent genetic and biochemical studies in *Anopheles gambiae* revealed a more complex role for cSPHs in the regulation of insect immune responses. Using the melanization of *Plasmodium berghei* ookinetes in *A. gambiae* midguts as a readout in functional genetic studies by RNA interference (RNAi), two distinct functional groups of cSPHs have been identified; cSPHs whose knockdown abolished ookinete melanization in a refractory mosquito genetic background are considered positive regulators and include CLIPA8 [12], SPCLIP1 (or CLIPA30) [28], and CLIPA28 [29], while those whose knockdown triggered ookinete melanization in susceptible mosquitoes are called negative regulators and include CLIPA2 [12] and CLIPA14 [30]. These positive and negative regulators also exhibit similar roles with respect to controlling PPO activation after systemic bacterial infections with *E. coli* [28–32], suggesting that they mediate core functions in the melanization immune response. Biochemical studies revealed that the infection-induced activation cleavage of most of these mosquito cSPHs is under the control of the

complement-like protein TEPI [28–30], a hallmark of mosquito immune effector responses against *Plasmodium* parasites [33, 34], bacteria [35–37], and fungi [38]. Downstream of TEPI, the sequential activation cleavage of SPCLIP1, CLIPA8, and CLIPA28 regulates the activity of cSPs in the cascade [29, 39]. SPCLIP1 and CLIPA2 also act as positive and negative regulators, respectively, of TEPI-mediated effector responses through unknown mechanisms, indicating that mosquito cSPHs exhibit more complex roles within and outside the context of melanization [28, 32]. Here, we characterize CLIPA7 as another positive regulatory cSPH that functions parallel to the TEPI-SPCLIP1-CLIPA8-CLIPA28 axis to drive the melanization of *E. coli* but not the Gram-positive bacteria *S. aureus* and *Micrococcus luteus*. We also show that CLIPA7 is recruited to bacterial surfaces and is essential for mosquito resistance to *S. aureus* infections in a melanization-independent manner. These results and the unique domain architecture of CLIPA7 among mosquito cSPHs suggest that in the context of the serine protease cascades that regulate melanization, certain cSPHs evolved pleiotropic roles that equip these cascades with functional plasticity much like the cascades that drive coagulation and complement activation in vertebrates.

## Materials and Methods

### *Anopheles gambiae* Rearing and Infections with *Plasmodium berghei*

All experiments were performed with adult female mosquitoes of *Anopheles gambiae* G3 strain. This strain has been established in our insectary in 2007 from the colony that existed at Imperial College London at that time. Mosquitoes were maintained at 27°C and 75% humidity with a 12-h day-night cycle. Larvae were reared in plastic pans and given Tetra Pond flakes or sticks for food. Adult mosquitoes were collected from larval pans, maintained on 10% sucrose solution, and given BALB/c mice blood for egg laying. Mice were anesthetized using ketamine/xylazine mixture solution. Mosquito infections with *P. berghei* (GFP-expressing strain PbG-FPCON) [40] were performed by allowing batches (corresponding to the different gene knockdowns) of 60 mosquitoes each to feed on 5- to 6-week-old anesthetized BALB/c mice infected with *P. berghei* at parasitemia levels of 4–6%, for approximately 15 min at 20°C. Mosquitoes were then maintained on 10% sucrose solution at 20°C until midguts were dissected at day 7 post-feeding on infected mice blood. Midguts were fixed in 4% formaldehyde for 30–40 min, washed with cold, 1× phosphate-buffered saline (PBS), and then mounted and imaged with a Leica upright fluorescence microscope to score the numbers of live GFP-expressing oocysts and dead melanized ookinetes, as previously described [29, 30]. Data were collected from three independent biological experiments, and statistical significance was calculated using Kruskal-Wallis test followed by Dunn's multiple comparison test, with *p* values <0.05 considered significant.

### Double-Stranded RNA Synthesis and Gene Silencing by RNAi

Double-stranded RNA (dsRNA) synthesis was performed using the T7 RiboMax Express Large-Scale RNA Production System (Promega) according to the manufacturer's instructions. DsRNAs were extracted with phenol:chloroform: isoamyl alcohol (25:24:1), precipitated with isopropanol and resuspended in nuclease-free water at a final concentration of 3.5 µg/µL. Primers used for dsRNA production are listed in online supplementary Table 1 (see [www.karger.com/doi/10.1159/000526486](http://www.karger.com/doi/10.1159/000526486) for all online suppl. material). In vivo gene silencing by RNAi was performed as previously described [41]. Briefly, 1–3-days-old female adult mosquitoes were anesthetized under CO<sub>2</sub> and microinjected intrathoracically with 69 nL of a 3.5 µg/µL gene-specific dsRNA solution in water (for single gene knockdown) or with 138 nL of a solution containing two different dsRNAs (each at a concentration of 3.5 µg/µL) for double gene knockdowns, using a Drummond Nanoject II Nanoliter injector. Mosquitoes were allowed 2–3 days to recover before further manipulation.

Efficiency of gene silencing was measured by Western blot analysis for all genes except Rel1 which was measured by quantitative real-time PCR (qRT-PCR) due to the lack of a Rel1-specific antibody. To measure the efficiency of gene silencing at the protein level, hemolymph was extracted from approximately 35 naïve mosquitoes per genotype including the ds*LacZ* control, at 3–4 days after dsRNA injection and proteins were quantified using Bradford Reagent (Fermentas). Equal amounts of proteins were resolved by nonreducing SDS-PAGE, transferred to immuno-blot PVDF membrane (Bio-Rad) using wet transfer (Bio-Rad), and subjected to Western blot analysis with the appropriate antibody dilution (see Western Blot Analysis section below). To measure gene silencing efficiency of Rel1 by qRT-PCR, total nucleic acids were extracted from 15 ds*LacZ* and ds*Rel1* mosquitoes using TRIzol reagent (Invitrogen), followed by chloroform extraction and precipitation by isopropanol. Contaminant genomic DNA was removed by treatment with the RNase-free DNase I (Thermo Scientific) as per the manufacturer's instructions. First-strand cDNA was produced from 1 µg of total RNA using the iScript cDNA synthesis kit (Bio-Rad) as described by the manufacturer. qRT-PCR was performed in a CFX96 Real-Time Detection System (Bio-Rad) using SYBR Green JumpStart Taq ReadyMix (Sigma), according to the manufacturer's instructions. The *A. gambiae* ribosomal *S7* gene was used as an internal control for normalization, and relative gene expression values were calculated using the comparative C<sub>T</sub> method. The following primers were used in qRT-PCR: AgS7-F: 5'-AGAACCAGCAGACCACCATC-3' and AgS7-R: 5'-GCTGCAA ACTTCGGCTATTC-3' [42]; Rel1-F: 5'-CCAACCTCGATCCGGTGTTC-3' and Rel1-R: 5'-TAG-GTCGGTTCGTGGAAAGTGA-3'.

### Survival and Microbial Proliferation Assays

The survival of dsRNA-treated adult female mosquitoes was scored over a period of 15 days after intrathoracic injection of a microbial suspension of ampicillin-resistant GFP-expressing *Escherichia coli* strain (OP-50) at an OD<sub>600</sub> of 0.8 [43] or chloramphenicol-resistant GFP-expressing *S. aureus* strain at an OD<sub>600</sub> of 0.8 [44] in PBS, or after spraying with a suspension of *Beauveria bassiana* (strain 80.2; a kind gift from D. Ferrandon) spores containing 10<sup>8</sup> spores/mL in 0.05% Tween-80, prepared as previously described [38, 45]. The Kaplan-Meier test was used to calculate the percent survival. Statistical significance of the observed differences

between the gene-specific dsRNAs and the ds*LacZ* control was calculated using the log-rank test. Experiments were repeated at least 3 times using different batches of mosquitoes and microbial cultures.

For the bacterial proliferation assays, dsRNA-treated mosquitoes were injected intrathoracically with 69 nL of the aforementioned *E. coli* and *S. aureus* strains (OD<sub>600</sub> = 0.8 for each). At 24 h post-bacterial challenge, a minimum of 4 batches of 8 mosquitoes each per genotype were grinded in 500 µL Luria-Bertani (LB) broth and serial dilutions of mosquito homogenates were plated onto LB agar plates containing the appropriate antibiotic to score the colony-forming units (CFUs). Data shown are from at least 5 independent biological experiments. Statistical analysis was performed using Kruskal-Wallis test followed by Dunn's multiple comparison test, with *p* values <0.05 considered significant.

The proliferation of *B. bassiana* in spore-injected mosquitoes was scored by qRT-PCR. Briefly, dsRNA-treated mosquitoes were injected each with approximately 30 *B. bassiana* spores suspended in water. Three days post-infection, 15 mosquitoes per genotype were grinded in liquid nitrogen with a mortar and pestle to create a fine powder. The powder was collected into Eppendorf Tubes, and genomic DNA was extracted in 2% cetyltrimethyl ammonium bromide buffer (Sigma), as previously described [29]. QRT-PCR was performed in a CFX96 Real-Time Detection System (Bio-Rad) using SYBR Green JumpStart Taq ReadyMix (Sigma), according to the manufacturer's instructions. *B. bassiana* primers and the calculation of the relative abundance of *B. bassiana* genomic DNA in the different mosquito genotypes have been previously described [29]. Data shown are from 5 independent biological experiments. Statistical significance of the observed differences was calculated using the Friedman test followed by Dunn's multiple comparison test.

### Western Blot Analysis

To monitor CLIPA7 protein dynamics in the hemolymph in response to systemic infections, hemolymph was collected by proboscis clipping from adult female mosquitoes at the indicated time points after injection with 69 nL containing either *E. coli* (OD<sub>600</sub> = 0.8) or *S. aureus* (OD<sub>600</sub> = 0.8) suspensions in PBS, 20 mg/mL suspension of pHrodo Green *E. coli* BioParticles (Invitrogen) in PBS, or 2,000 *B. bassiana* spores. The same infection protocol was used to monitor the effects of CLIPA7 kd on the cleavage profiles of CLIPA8 and CLIPA28. To monitor CLIPA7 protein dynamics in ds*SRPN2* mosquitoes, hemolymph was collected from the indicated naïve mosquito genotypes at 7 days post-dsRNA injection. In all conditions, hemolymph was collected from 35 mosquitoes per sample directly into ice-chilled PBS containing a protease inhibitor cocktail (Roche). Protein quantification in hemolymph samples was performed using the Bradford protein assay (Fermentas) to ensure equal protein loading on the gel for all samples in a given experiment. Hemolymph samples were resolved by reducing SDS-PAGE and transferred to immunoblot PVDF membranes by wet transfer (Bio-Rad). Primary antibodies used for immunoblotting are affinity-purified rabbit αCLIPA7 (produced by Boster Bio), affinity-purified rabbit αCLIPA8 (produced by Boster Bio), affinity-purified rabbit αCLIPA28 [29], rabbit αPPO6 [46], rabbit αSRPN3 [47], and mouse αApoII [48] added overnight at the following dilutions 1:4,000, 1:1,000, 1:100, 1:2,000, 1:1,000, and 1:100, respectively. Affinity-purified αTEP1, αCTL4, αSPCLIP1 antibodies (produced by Boster Bio) and αCLIPC9 (kind gift from M.

Povelones) were used at 1:2,000, 1:1,000, 1:2,000, and 1:2,000, respectively, to determine the efficiency of knockdown of the respective genes in hemolymph extracts from naïve mosquitoes, as described above. All custom-made antibodies produced by Boster Bio were affinity purified by the manufacturer using long peptides specific to the indicated proteins. Following washing, blots were incubated for 1 h with anti-mouse or anti-rabbit IgG horseradish peroxidase-conjugated secondary antibodies at dilutions of 1:6,000 and 1:12,000, respectively. Blots were then washed, immersed in Bio-Rad Clarity Max Western ECL substrate, and imaged using ChemiDoc MP System (Bio-Rad). Where indicated, band quantification was performed using Image Lab software. All Western blot experiments were repeated at least 3 times.

The localization of CLIPA7 to *E. coli* bioparticles (Invitrogen) was performed using the bioparticle surface extraction exactly as previously described [28]. Briefly, commercial *E. coli* bioparticles (20 mg/mL) were injected intrathoracically into female adult mosquitoes and hemolymph was extracted 20 min after injection. Bioparticles were separated from the hemolymph by centrifugation to collect the soluble fraction; then, pellets were incubated with (1×) denaturing Laemmli buffer to elute their surface-bound proteins (bound fraction). Proteins in the soluble and bound fractions were resolved by nonreducing SDS-PAGE, and Western blot was performed as described above. Blots were probed with rabbit αCLIPA7 (1:4,000).

#### Melanization-Associated Spot Assay

Melanization-associated spot assay (MelASA) was performed using 35 dsRNA-treated mosquitoes that were infected by intrathoracic injection with *E. coli* (OD<sub>600</sub> = 0.8 or 3), *S. aureus* (OD<sub>600</sub> = 0.8), or *M. luteus* (OD<sub>600</sub> = 2) and housed for 12 h in paper cups containing freshly inserted white filter paper (Whatman, 55 mm diameter). After 12 h, filter papers were imaged in a ChemiDoc MP System (Bio-Rad) using Image Lab software. Image processing and spot area quantification were performed using ImageJ software exactly as previously described [39]. Statistical analysis was performed using one-way ANOVA followed by Dunn's multiple comparison test, with *p* values <0.05 considered significant.

#### Immunofluorescence Assays

Abdomens were dissected from adult female mosquitoes at 20–30 min after intrathoracic injection of GFP-expressing *S. aureus* (OD<sub>600</sub> = 2), GFP-expressing *E. coli* (OD<sub>600</sub> = 2), *Bacillus cereus* (OD<sub>600</sub> = 2), or *M. luteus* (OD<sub>600</sub> = 2). Abdomens were fixed for 20 min in 2% formaldehyde (Polysciences Inc.), then washed with PBS, and blocked for 1 h in PBS containing 2% bovine serum albumin and 0.03% Triton X-100. Tissues were incubated overnight with the following affinity-purified, primary rabbit antibodies, αCLIPA7, αCLIPA8, and αSPCLIP1 at the following dilutions 1:1,300, 1:300, and 1:300, respectively. Abdomens were washed with PBS containing 0.03% Triton X-100 (PBS-T), incubated with anti-rabbit Alexa 568 antibody for 1 h (1:800 dilution), then washed with PBS-T, stained with Hoechst stain (Invitrogen), and mounted.

Hemocyte perfusions were performed from 50 mosquitoes at 20–30 min after intrathoracic injection of GFP-expressing *S. aureus* (OD<sub>600</sub> = 2) or *E. coli* (OD<sub>600</sub> = 2). Hemolymph was extracted in 5 μL PBS supplemented with a protease inhibitor cocktail, deposited on VistaVision HistoBond Microscope Slides (VWR), and allowed to dry partially for around 20 min. Hemocytes were then

fixed for 10 min in 2% formaldehyde (Polysciences Inc.), then washed with PBS, and blocked for 1 h in PBS containing 2% bovine serum albumin and 0.01% Triton X-100. Hemocytes were incubated overnight with αCLIPA7 at 1/1,300, then washed with PBS-T, and incubated with anti-rabbit Alexa 568 antibody for 1 h (1/800 dilution). Following washing, nuclei were stained with Hoechst (Invitrogen) and cells topped with mounting medium. Images were acquired on Zeiss LSM 710 confocal and Leica upright fluorescence microscopes.

## Results

### *CLIPA7 Contributes to the Melanization Immune Response in a Microbial Class-Dependent Manner*

CLIPA7 is an unusually large cSPH that was previously shown to function as a weak negative regulator of the melanization response to *P. berghei* ookinetes, in the context of a functional genetic screen of *A. gambiae* cSPHs and cSPs; *CLIPA7* kd in the susceptible G3 *A. gambiae* strain triggered the melanization of approximately 16.9% of ookinetes [12]. To further address the role of CLIPA7 in the melanization response, we assessed the effect of CLIPA7 silencing on the melanotic response to septic *E. coli* infections using the MelASA that measures the brown melanotic material excreted by mosquitoes onto filter papers lining the bottom of their housing cups, and which was shown to be reflective of the hemolymph phenoloxidase activity [39]. Mosquitoes treated with gene-specific dsRNA for CLIPA7 (*dsCLIPA7*) were injected intrathoracically with *E. coli* (OD<sub>600</sub> = 0.8 or 3), and total spot area of excreta on filter papers (online suppl. Fig. 1, 2) was measured by ImageJ as previously described [39]. Mosquitoes treated with dsRNA for the β-galactosidase gene (*dsLacZ*) and SPCLIP1, a key positive regulator of melanization [28], were used as negative and positive controls, respectively. The results showed that *CLIPA7* kd significantly reduced the melanization response to *E. coli* at both, the lower and high ODs, a phenotype similar to that of SPCLIP1 (Fig. 1a). However, *CLIPA7* kd did not alter the melanization response to *S. aureus* nor to *M. luteus* infections in contrast to *SPCLIP1* kd which reduced it significantly (Fig. 1b; online suppl. Fig. 3, 4), suggesting that CLIPA7 may be dispensable for the melanization of Gram-positive bacteria.

The observed positive regulatory role of CLIPA7 in *E. coli* melanization was surprising since it contradicted its previously reported role as a negative regulator of *P. berghei* melanization [12]. Hence, we readdressed the role of CLIPA7 in *P. berghei* melanization. Silencing CLIPA7 in our susceptible wild-type G3 mosquitoes did not trigger

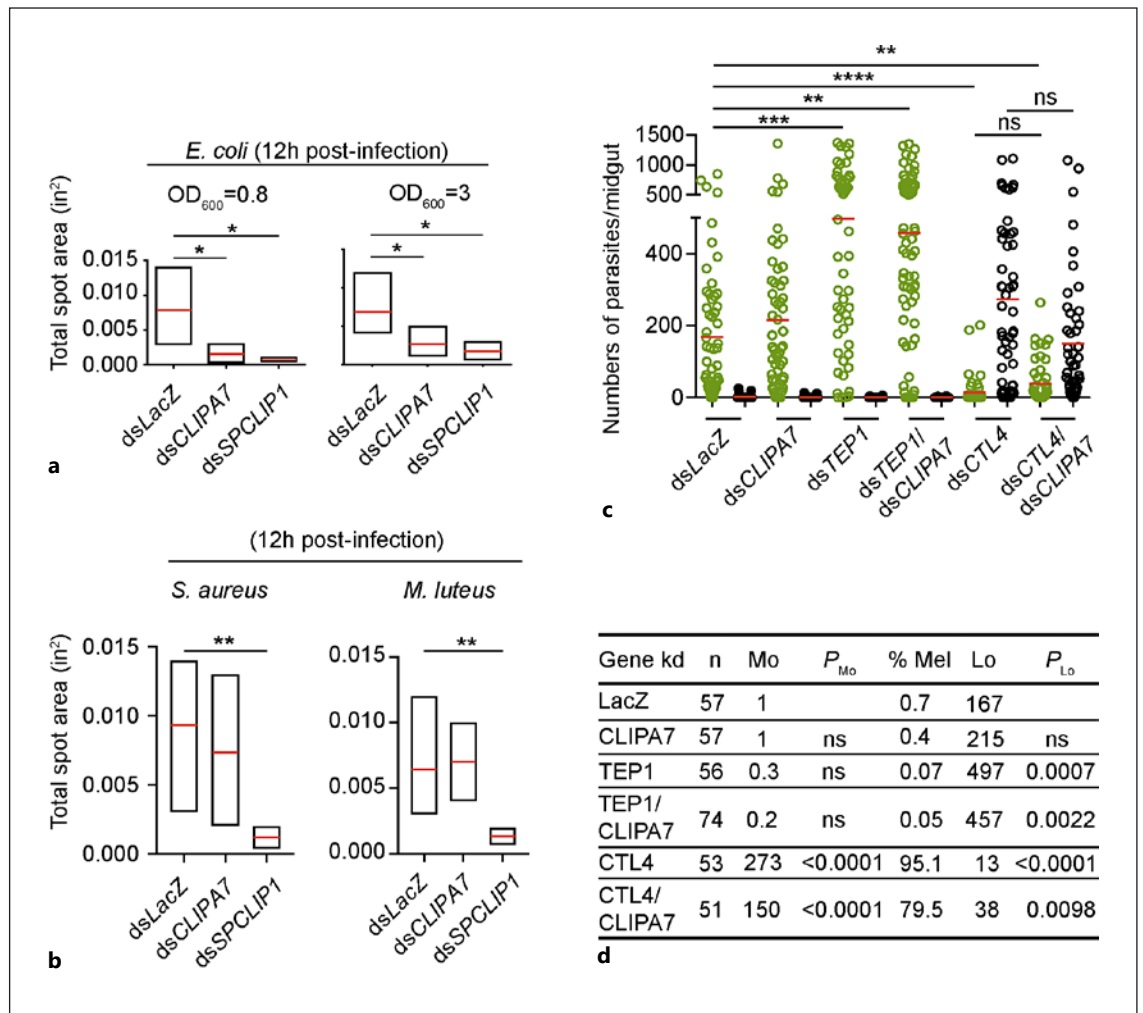


**Fig. 1.** CLIPA7 is a positive regulator of the melanization response. MelASA of the indicated mosquito genotypes at 12 h post-injection of *E. coli* (OD<sub>600</sub> = 0.8 and 3) (**a**) and *S. aureus* (OD<sub>600</sub> = 0.8) and *M. luteus* (OD<sub>600</sub> = 2) (**b**). Red lines indicate mean values. Data shown are from at least five independent biological experiments. **c** Scatter plots of live GFP-expressing *P. berghei* oocysts (green circles) and dead melanized ookinetes (black circles) scored in the midguts of the indicated mosquito genotypes at 7 days post-infection. Red lines indicate mean values. Data shown are from three independent biological experiments. Statistical analysis for MelA-

SA and parasite distribution were performed using one-way ANOVA and Kruskal-Wallis test, respectively, followed by Dunn's multiple comparison test, with *p* values <0.05 considered significant. **d** Tabulated data of **c** showing the percentages of melanized ookinetes (% Mel), and the mean numbers of melanized ookinetes (Mo) and live oocysts (Lo) per midgut. The *p* values for the distribution of melanized and live parasites in each genotype with respect to dsLacZ are shown. \**p* < 0.05; \*\**p* < 0.01; \*\*\**p* < 0.001; \*\*\*\**p* < 0.0001; ns, nonsignificant, in<sup>2</sup>, inch square.

the melanization of *P. berghei* ookinetes; the numbers of melanized ookinetes and live oocysts were similar to those in dsLacZ control (Fig. 1c, d; online suppl. Table 2). Silencing CLIPA7 in the highly melanotic dsCTL4 G3 mosquitoes [49] induced a small but insignificant decrease in the numbers of melanized ookinetes as compared to dsCTL4 control (Fig. 1c, d); the numbers of live oocysts also did not differ significantly between dsCTL4 and dsCLIPA7/dsCTL4 mosquitoes. These results indi-

cate that CLIPA7 is not involved in *P. berghei* melanization, neither as a negative nor as a positive regulator, which contradicts its previously reported role as a weak negative regulator of ookinete melanization [12]. This prompted us to re-assess the specificity of the old dsRNA template used to silence CLIPA7 in our previous study. A BLAST analysis of the gene sequence corresponding to this old template against the latest mosquito annotation in VectorBase (vectorbase.org) identified a sequence that

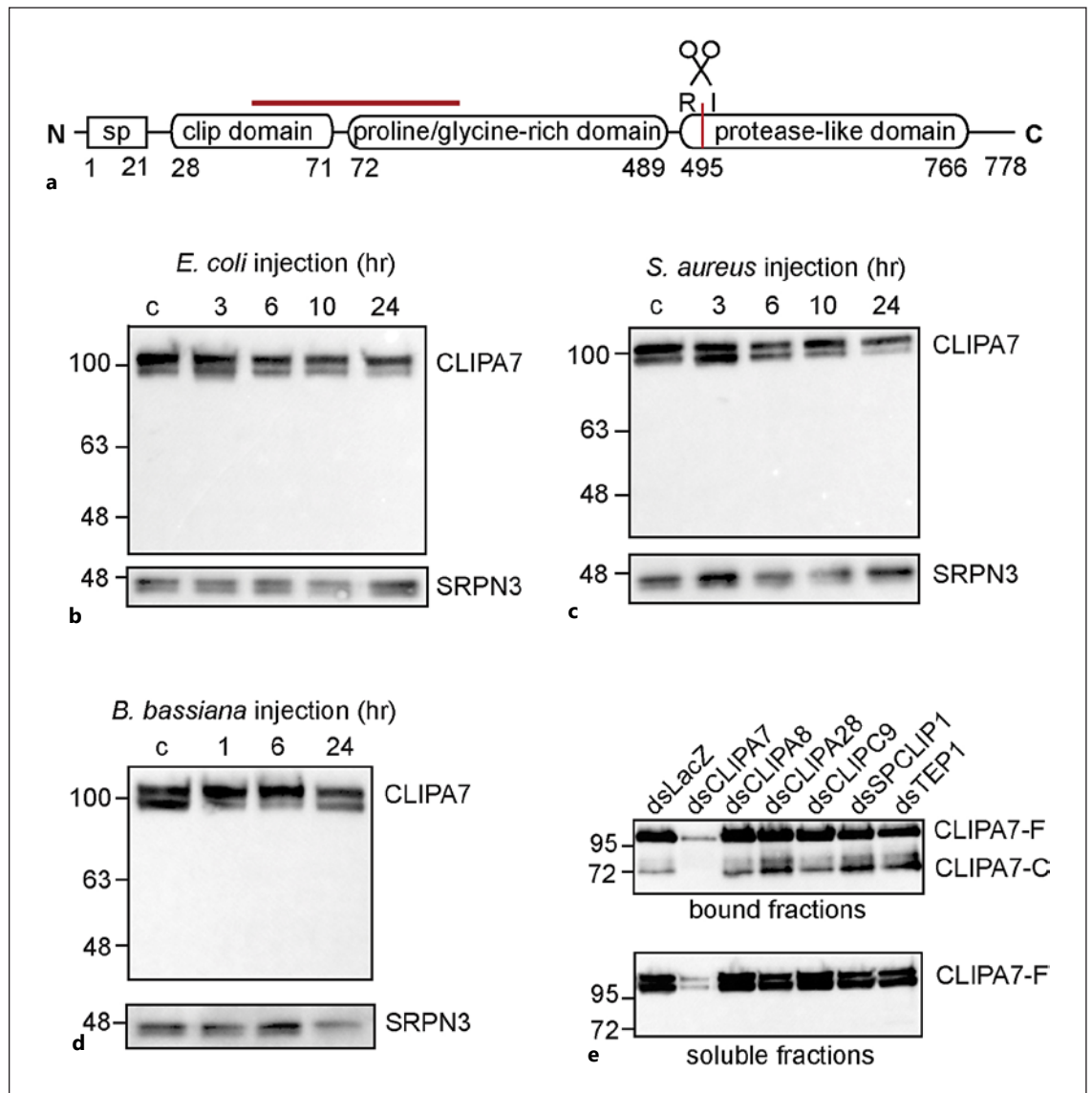


**Fig. 2.** CLIPA7 is not cleaved following septic infections. **a** Schematic representation of CLIPA7 protein with its constituent domains. Numbers refer to amino acid residues at the start/end of each domain. The predicted cleavage site after an arginine (R) at the beginning of the protease domain is indicated by scissors. The red line corresponds to the peptide sequence against which antibodies were raised. Western blots showing CLIPA7 protein in hemolymph extracts of wild-type mosquitoes at the indicated time points after injection with *E. coli* ( $OD_{600} = 0.8$ ) (**b**), *S. aureus* ( $OD_{600} = 0.8$ ) (**c**), and *B. bassiana* (2,000 spores/mosquito) (**d**). In all blots, each lane contained hemolymph extracts from 35 mos-

quitoes. Membranes were probed with  $\alpha$ SRPN3 as loading control. The shown blots are representative of at least three independent experiments. **e** Hemolymph containing *E. coli* bioparticles was extracted from the indicated mosquito genotypes at 20 min after bioparticle injection into the hemocoel. Bioparticles were pelleted by centrifugation, and the soluble fractions collected. Bound proteins were extracted from bioparticle pellets with Laemmli protein loading buffer (1 $\times$ ). Shown is a Western blot analysis of the soluble and bound fractions. The image is representative of two independent experiments. sp, signal peptide.

matches CLIPA14, a key negative regulator of *P. berghei* melanization [30], in 34 contiguous nucleotides containing only 1 nucleotide mismatch (online suppl. Fig. 5). Hence, the weak *P. berghei* melanization phenotype as-

sociated with CLIPA7 kd in our previous study is most likely attributed to an off-target effect that weakly silenced CLIPA14. It is worth noting that CLIPA14 was absent from the initial list of *A. gambiae* annotated genes

[50] based on which our earlier genetic screen was performed. Gene silencing efficiencies of TEP1 and SPCLIP1 are shown in online supplementary Figure 6b and d, respectively.

*Proteolysis within the SPCLIP1-CLIPA8-CLIPA28 cSPH Module Is Not Regulated by CLIPA7*

SPCLIP1 [28], CLIPA8 [12, 31], and CLIPA28 [29] are three cSPHs that act downstream of TEP1 and are essential for the melanization response to *Plasmodium* and systemic bacterial infections. These cSPHs are rapidly cleaved following septic infections of the hemolymph, a feature that was exploited in gene silencing experiments coupled with Western blot analysis to place them in a functional module displaying a clear hierarchy of activation, with SPCLIP1 acting most upstream followed by CLIPA8 and then CLIPA28 [29, 39]. Since CLIPA7 is also required for the *E. coli*-induced melanization response, we first assessed whether CLIPA7 exhibits an infection-induced cleavage profile that can be used as a readout to facilitate its placement with respect to the above cSPHs. Western blot analysis of hemolymph extracts collected at several time points after mosquito injections with *E. coli* (Fig. 2b; online suppl. Fig. 7a), *S. aureus* (Fig. 2c; online suppl. Fig. 7b), and *B. bassiana* spores (Fig. 2d; online suppl. Fig. 7c) revealed a double band at approximately 100 kDa corresponding to full-length CLIPA7 with no detection of a cleaved protein product, whereas the theoretical (predicted) molecular weight of CLIPA7 is approximately 77 kDa.

We fortuitously identified a cleaved product of CLIPA7 while investigating the recruitment of CLIPA7 to *E. coli* bioparticles, using our previously described bioparticle surface extraction assay [28, 32]. Using this assay, we have previously shown that SPCLIP1, CLIPA2, and CLIPA14 are recruited to bacterial surfaces and that, for the two former cSPHs, it was TEP1-dependent [28, 30, 32]. Western blot analysis of the bound fractions revealed a band at ~100 kDa corresponding to full-length CLIPA7 and another at ~72 kDa corresponding to the proteolytically processed form (Fig. 2e; online suppl. Fig. 7d). The higher molecular weight band was strongly reduced, and the lower was depleted in the dsCLIPA7 sample confirming the specificity of the observed bands. CLIPA7 is predicted to be cleaved after Arginine 513 at the beginning of the protease-like domain (Fig. 2a; [5]) generating N-terminal and C-terminal fragments with theoretical molecular weights of ~45 and ~30 kDa, respectively, under reducing conditions. Of note, the CLIPA7 antibody was raised against a long peptide sequence in the N-terminus

of the protein spanning most of the clip and part of the proline/glycine-rich domains; hence, it does not recognize the smaller C-terminal fragment containing the protease-like domain. The observed aberrant migrations of full-length and cleaved CLIPA7 relative to their corresponding theoretical weights are most likely due to the low prevalence of hydrophobic amino acid residues in the protein resulting in lower SDS binding and consequently lower mobility, compared to other proteins with more hydrophobic residues. Indeed, the grand average of hydropathy (GRAVY) index score of CLIPA7 is  $-0.485$  [51], indicating that it is significantly hydrophilic. This aberrant migration has been observed for other proteins with low GRAVY scores such as collagen peptides that are also rich in glycine residues [52]. Interestingly, neither TEP1 silencing nor the silencing of CLIPA8, CLIPA28, or SPCLIP1 rescued CLIPA7 cleavage (Fig. 2e; online suppl. Fig. 7d). Silencing CLIPC9, a recently identified cSP with essential roles in *Plasmodium* and bacterial melanization [39] also failed to rescue CLIPA7 cleavage. The fact that the cleaved form of CLIPA7 was not detected in the soluble fractions suggests that it is generated locally on microbial surfaces to which it remains tightly associated. It is worth noting that the cleaved form of CLIPA7 was not detected systematically in all experiments involving challenges with bioparticles.

Next, we asked whether CLIPA7 acts upstream of the SPCLIP1-CLIPA8-CLIPA28 module by gauging the effect of CLIPA7 kd on the infection-induced activation cleavage profiles of CLIPA8 and CLIPA28. CLIPA7 kd failed to rescue the cleavage of CLIPA8 (Fig. 3a, c, e; online suppl. Fig. 8a, c, e) and CLIPA28 (Fig. 3b, d, f; online suppl. Fig. 8b, d, f) in response to mosquito injections with *E. coli*, *S. aureus*, and *B. bassiana* spores, respectively. On the other hand, CLIPA8 kd almost completely rescued CLIPA28 cleavage (Fig. 3b, d, f) in all three infections, confirming our previous observations of the downstream position of CLIPA28 in the module [29]. Altogether, our results indicate that CLIPA7 does not act neither upstream nor downstream of the SPCLIP1-CLIPA8-CLIPA28 module.

*CLIPA7 Loss in SRPN2 kd Mosquitoes Is Not Rescued by Silencing CLIPA8 or CLIPA28*

SRPN2 is a key negative regulator of the mosquito melanization response whose knockdown triggers a potent melanotic response against *Plasmodium* ookinetes, and substantial spontaneous tissue melanization in naïve mosquitoes associated with a strong reduction in hemolymph PPO protein levels at later time points [53]. We

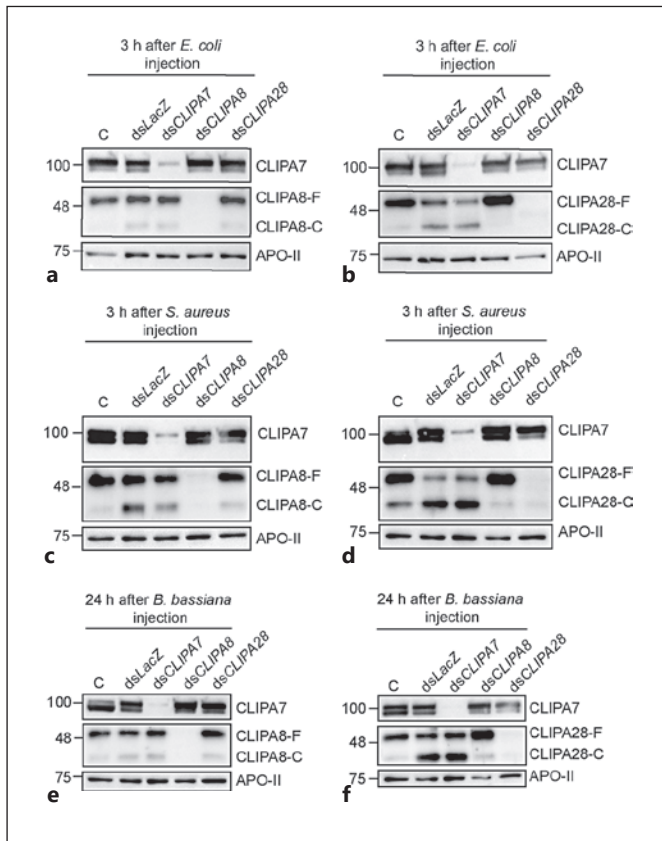


**Fig. 3.** CLIPA7 is not required for the activation cleavage of CLIPA8 and CLIPA28. Western blots showing CLIPA8 (a) and CLIPA28 (b) cleavage in hemolymph extracts from the indicated mosquito genotypes at 3 h after *E. coli* ( $OD_{600} = 0.8$ ) injection. Western blots showing CLIPA8 (c) and CLIPA28 (d) cleavage in hemolymph extracts from the indicated mosquito genotypes at 3 h after *S. aureus* ( $OD_{600} = 0.8$ ) injection. Western blots showing CLIPA8 (e) and CLIPA28 (f) cleavage in hemolymph extracts from the indicated mosquito genotypes at 24 h after *B. bassiana* injection (2,000 spores/mosquito). In all blots, each lane contained hemolymph extracts from 35 mosquitoes. Membranes were also probed with  $\alpha$ CLIPA7, and with  $\alpha$ -Apolipoprotein II ( $\alpha$ ApoII) as loading control. The blots shown are representative of at least three independent experiments.

recently showed that, in addition to PPO, *SRPN2* kd in naïve mosquitoes also reduced significantly the hemolymph levels of CLIPA8 and CLIPA28, suggesting that the spontaneous melanotic reaction triggered in those mosquitoes most likely consumes several hemolymph proteins involved in this response [29]. Similarly, we observed a strong reduction in CLIPA7 protein in the hemolymph of ds*SRPN2* naïve mosquitoes at 7 days after dsRNA injection relative to the ds*LacZ* controls of the same age, indicating that CLIPA7 is also consumed dur-

ing that reaction (Fig. 4; online suppl. Fig. 9). The loss of CLIPA7 in ds*SRPN2* naïve mosquitoes was not rescued by the silencing of CLIPA8, CLIPA28, SPCLIP1 nor TEPI1, further supporting our previous observations that these factors do not seem to function upstream of CLIPA7.

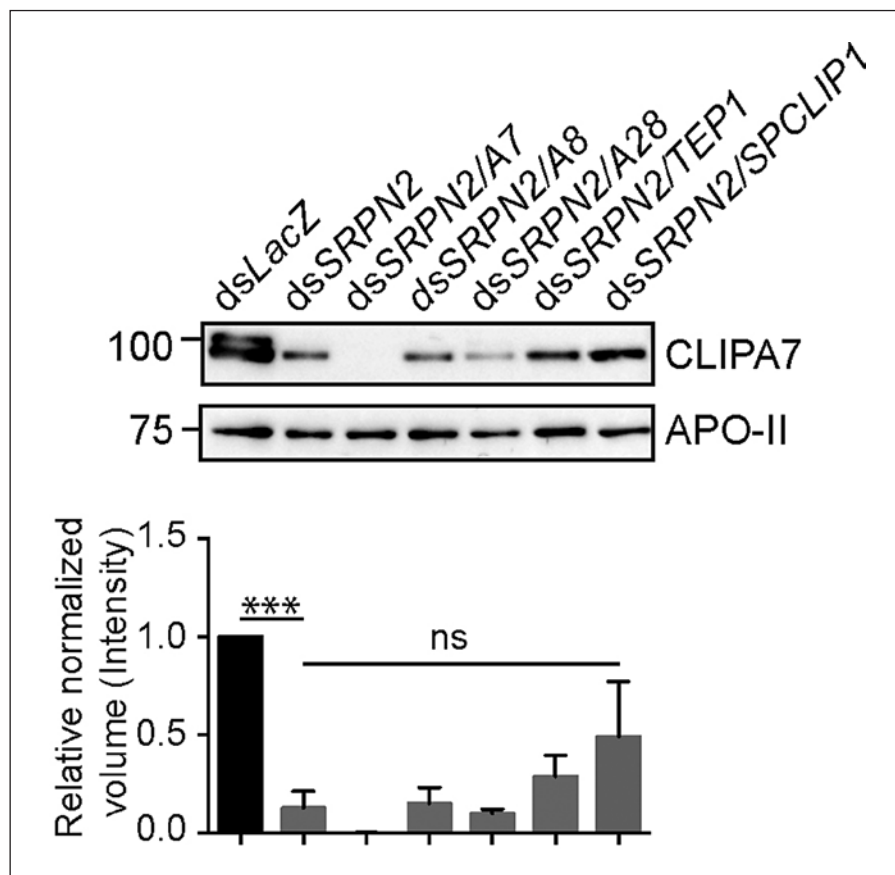
### CLIPA7 Contributes to Antimicrobial Defense

cSPs in insects are major components of cascades that activate not only the melanization response but also the Toll immune pathway which provides protection against systemic infections with different classes of microbes [54–57]. To determine whether CLIPA7 is essential for mosquito immune defense, we scored the effect of silencing CLIPA7 on the ability of mosquitoes to endure and resist microbial challenges. Endurance was measured by scoring the survival of ds*CLIPA7* mosquitoes in response to infections with *E. coli*, *S. aureus*, and *B. bassiana*. Silencing CLIPA7 did not compromise mosquito survival to systemic infections with *E. coli* and *S. aureus*, whereas silencing the respective positive controls *CTL4* [31, 58] and the NF- $\kappa$ B-like transcription factor *Rel1* [6] did (Fig. 5a, b). However, infections with the entomopathogenic fungus *B. bassiana* compromised the survival of ds*CLIPA7* mosquitoes (Fig. 5c) to a similar extent as that of ds*TEPI1*, used herein as positive control [38]. Next, we asked whether silencing CLIPA7 alters mosquito resistance to infection by scoring microbial proliferation in whole mosquitoes. Ds*CLIPA7* mosquitoes injected with *E. coli* exhibited similar levels of bacterial proliferation in their tissues as ds*LacZ* control (Fig. 5d), whereas significant proliferation was observed in ds*CTL4* mosquitoes, as previously reported [31, 58]. In contrast, ds*CLIPA7* mosquitoes exhibited significantly enhanced proliferation of *S. aureus* (Fig. 5e), suggesting that CLIPA7 is implicated in the immune-mediated clearance of this bacterium. With respect to *B. bassiana* infections, ds*CLIPA7* mosquitoes showed mixed phenotypes characterized by increased fungal proliferation in certain experiments (though not to the same extent as ds*TEPI1* mosquitoes) but not in others, in contrast to ds*TEPI1* mosquitoes which consistently exhibited an increase in *B. bassiana* proliferation (Fig. 5f), as previously reported [29].

### CLIPA7 Is Recruited to Bacterial Surfaces

The involvement of CLIPA7 in *S. aureus* clearance and in the melanization of *E. coli* prompted us to characterize whether CLIPA7 function requires its localization to bacterial surfaces by performing a series of immunohistochemical staining of female mosquito tissues at 20 min

**Fig. 4.** CLIPA7 consumption in *SRPN2* kd naïve mosquitoes is not rescued by the knockdown of positive regulatory cSPHs nor TEP1. Representative Western blot showing CLIPA7 protein levels in hemolymph extracts from the indicated naïve mosquito genotypes at day 7 after dsRNA injection. Hemolymph was extracted from 35 mosquitoes per sample. Protein quantification was performed using Bradford assay, and equal amounts of hemolymph proteins were loaded per lane. Membranes were also probed  $\alpha$ ApoII as loading control. Densitometric analysis of protein bands by Image Lab software from four independent experiments. Intensities of CLIPA7 bands were quantified by densitometry and normalized to those of ApoII bands after background subtraction. Shown are the normalized volumes (intensities) expressed relative to the normalized CLIPA7 volume in *dsLacZ* as reference point. Statistical analysis was performed using Student's *t* test. \*\*\**p* < 0.005; ns, nonsignificant.



after intrathoracic bacterial injections. The rationale behind conducting these assays at an early time point is to maximize the chance of imaging free bacteria (i.e., not phagocytosed), as the majority of bacteria risk to be cleared by phagocytes at later time points. CLIPA7 showed clear localization to GFP-expressing *S. aureus* cells in perfused hemolymph (Fig. 6a) and in dissected abdomens (Fig. 6b). The fact that CLIPA7-labeled *S. aureus* cells retained their cytosolic GFP signal suggests that these cells were viable. We also observed CLIPA7 labeling of GFP-expressing *E. coli* cells in dissected abdomens (Fig. 6c), indicating that CLIPA7 localizes to both Gram types. To determine whether this pattern of localization is CLIPA7-specific or is a general feature of cSPHs with immune phenotypes, we gauged the interaction of CLIPA8 and SPCLIP1, two key cSPHs in the melanization response, with the same *S. aureus* strain. Neither CLIPA8 (Fig. 6d) nor SPCLIP1 (Fig. 6e) was detected on the GFP-expressing *S. aureus* cells. Confocal microscopy imaging of perfused hemolymph revealed hemocytes as the main producers of CLIPA7 as well as a pattern of CLIPA7 staining of *S. aureus* cells identical to that observed with clas-

sical fluorescence microscopy (Fig. 6f). Western blot analysis detected CLIPA7 protein in hemolymph and abdomen extracts but not in midgut extracts (online suppl. Fig. 10), further supporting that hemocytes, most likely circulating and sessile, are the main producers of CLIPA7.

To exclude the possibility that the observed CLIPA7 staining could be somehow influenced by the GFP-expressing nature of the transgenic *E. coli* and *S. aureus* strains used in these assays, we probed the interaction of CLIPA7 with 3 other non-GFP-expressing strains of *S. aureus* (Fig. 7a), *B. cereus* (Fig. 7b), and *M. luteus* (Fig. 7c) in dissected abdomens of female mosquitoes injected with these bacteria. CLIPA7 was detected on melanized and nonmelanized cells of these bacteria, indicating that it exhibits a broad pattern of interaction with bacterial surfaces.

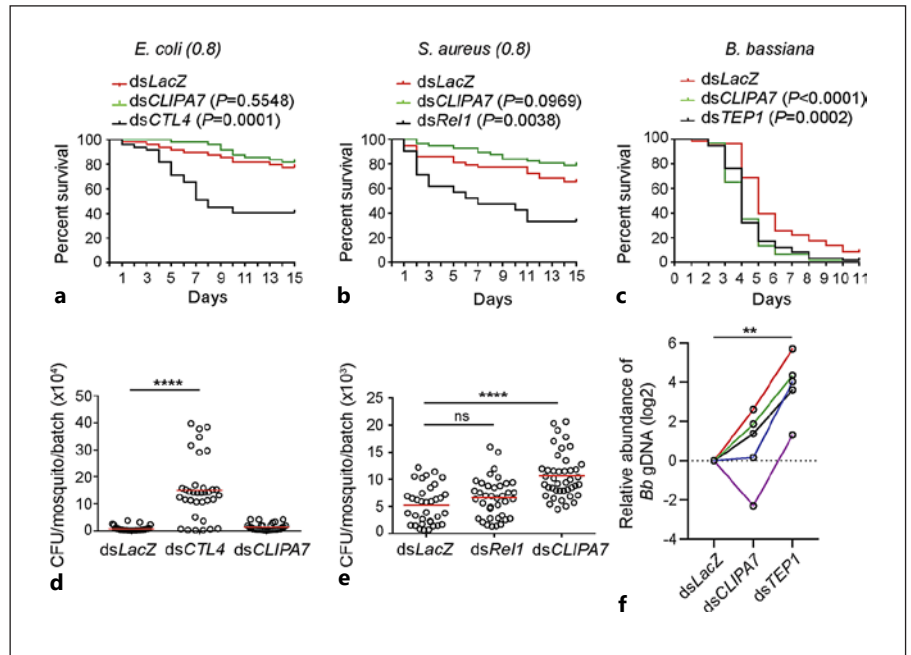


**Fig. 5.** CLIPA7 contributes to antimicrobial defense. Survival assays of the indicated mosquito genotypes following injection with *E. coli* (OD<sub>600nm</sub> = 0.8) (**a**), *S. aureus* (OD<sub>600nm</sub> = 0.8) (**b**), and after spraying with a *B. bassiana* suspension of 1 × 10<sup>8</sup> spores/mL (**c**). One representative experiment is shown from at least three independent biological experiments. The Kaplan-Meier survival test was used to calculate the percent survival. Statistical significance of the observed differences was calculated using the log-rank test, with *p* values <0.05 considered significant. Bacterial proliferation assays conducted on mosquitoes injected with *E. coli* (OD<sub>600nm</sub> = 0.8) (**d**) and *S. aureus* (OD<sub>600nm</sub> = 0.8) (**e**). Batches of 8 whole mosquitoes each were grinded in LB medium at 24 h after infection, and colony-forming units (CFUs) were scored on LB plates supplemented with the appropriate antibiotic. Each point on the scat-

ter plot represents the mean CFU per mosquito per batch. Means are shown as red lines. Statistical analysis was performed using Kruskal-Wallis test followed by Dunn's multiple comparison test, with *p* values <0.05 considered significant. \*\*\*\**p* < 0.0001. Data shown for *E. coli* and *S. aureus* are from 5 to 7 independent biological experiments, respectively. **f** Relative abundance of *B. bassiana* genomic DNA was measured by qRT-PCR in the indicated mosquito genotypes at day 3 after spore injection. Each point on the graph represents the mean relative abundance of *B. bassiana* genomic DNA in total DNA extracted from a batch of 15 mosquitoes. Five different biological experiments are shown, each in a different color. Statistical significance of the observed differences was calculated using the Friedman test followed by Dunn's multiple comparison test. \*\**p* < 0.01.

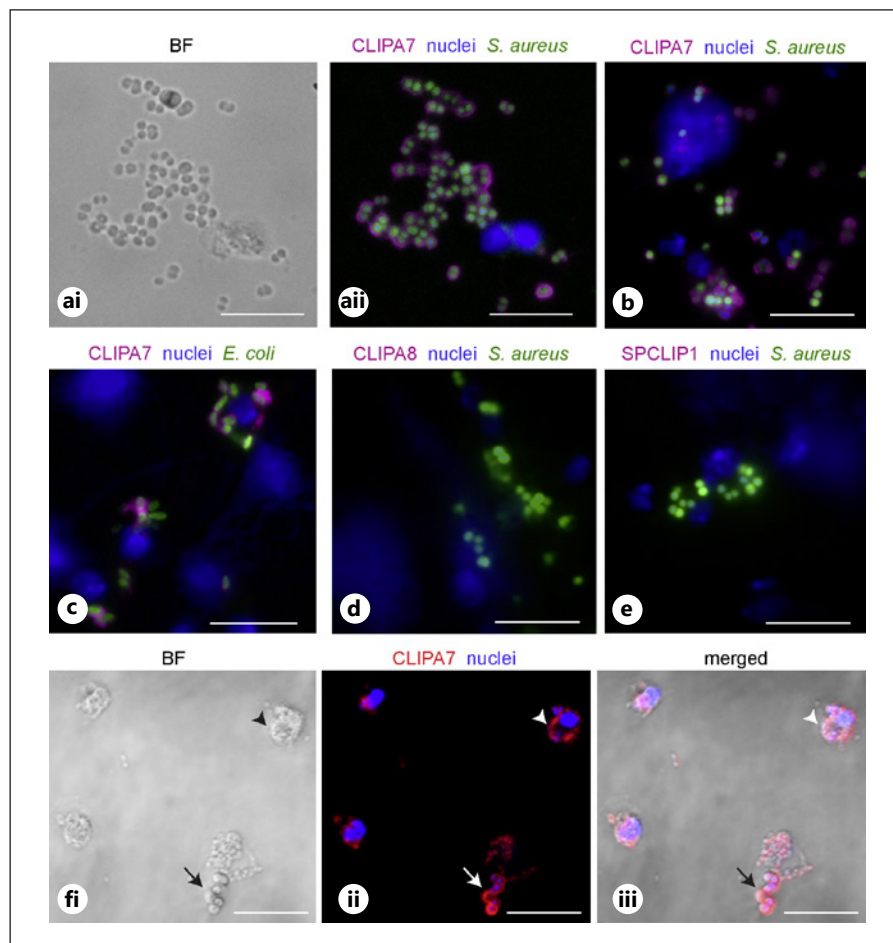
## Discussion

The melanization response in insects is regulated by complex serine protease cascades composed of cSPHs, cSPs, and their regulatory serpins. In *A. gambiae*, TEP1 acts as the most upstream trigger of the melanization response elicited against *Plasmodium* parasites, bacteria, and fungi [28, 29, 33, 38]. Downstream of TEP1, the SP-CLIP1-CLIPA8-CLIPA28 core module of cSPHs plays an essential role in the infection-induced melanization response [29, 39]. This module acts upstream of and controls the proteolytic activation of CLIPC9 which was also shown to be required for microbial melanization [39]. Our biochemical analysis suggests that CLIPA7 does not belong to the TEP1-cSPH core module-CLIPC9 axis but rather acts parallel to it in regulating the melanization of

*E. coli*. It was surprising to note that CLIPA7 cleavage is TEP1-independent, as this is the first example of an cSPH required for melanization but eludes TEP1 control. These results further support the existence of parallel axes that converge on *E. coli* melanization: an axis controlled by TEP1 and another involving CLIPA7. What factor(s) control proteolytic activation within the CLIPA7 axis remains to be determined.

The fact that CLIPA7 is required for *E. coli* but not *P. berghei* and *S. aureus* melanization is an interesting observation that points to microbial class-specific functions associated with certain components of these protease cascades. So far, all the key regulators of the infection-induced melanization response including TEP1, SPCLIP1, CLIPA8, CLIPA28, and CLIPC9 exhibit a broader role involving *E. coli* and *P. berghei* [12, 28, 29, 31–33, 39],

**Fig. 6.** CLIPA7 localizes to the surfaces of *E. coli* and *S. aureus*. Immunofluorescence assays showing CLIPA7 labeling of GFP-expressing *S. aureus* (OD<sub>600</sub> = 2) in **a** perfused hemolymph and **b** dissected abdomens, and **c** of GFP-expressing *E. coli* (OD<sub>600</sub> = 2) in dissected abdomens. Labeling of GFP-expressing *S. aureus* (OD<sub>600</sub> = 2) in dissected abdomens with CLIPA8 (**d**) and SPCLIP1 (**e**), respectively. Nuclei (blue) were stained with Hoechst. **f** Confocal microscope section (1 μm thick) of perfused hemolymph showing CLIPA7 staining of *S. aureus* cells (arrows) and CLIPA7 production by hemocytes (arrowheads). Scale bars correspond to 10 μm. All images were taken on a Leica upright fluorescence microscope (except **f**) and are representative of at least 2 independent biological experiments. BF, bright field.



with TEP1 and CLIPA8 also involved in fungal melanization [38]. However, the role of all of these regulators in the melanization of Gram-positive bacteria has not been addressed yet, with the exception of SPCLIP1 whose involvement in *S. aureus* melanization has been established in this study. The CLIPA7 phenotype informs future studies to assess *E. coli* and *S. aureus* melanization in parallel as readouts to better characterize immunity genes implicated in that response and to understand at what level functional specialization emerges in these cascades. This functional specialization has been addressed in mosquitoes mainly in the context of *Plasmodium* and tissue melanization [59, 60]. The recent observation that TEP1 is required for *P. berghei* but not *P. falciparum* melanization in CTL4 knockout mosquitoes stresses the importance of using a broader panel of microbes to better characterize this response [61].

We were not able to detect the cleaved form of CLIPA7 in hemolymph extracts of mosquitoes injected with live

bacteria even at high OD values of 3 (data not shown). Only by injecting commercial *E. coli* bioparticles, the cleaved form was detected, though not systematically. These observations suggest that a fraction of the cleaved, active form of CLIPA7 may be either circulating in the hemolymph from where it is rapidly cleared or that the active form is stably associated with the surfaces of microbes that become trapped in a melanin coat or cleared by phagocytes. The fact that in the bioparticle surface extraction assay the processed form of CLIPA7 was only observed in the bound but not the soluble fraction supports a tight association with microbial surfaces. In instances where we have succeeded in detecting cleaved forms of cSPHs including CLIPA8 [31], CLIPA28 [29], and CLIPA14 [30], it is likely because these forms leach from microbial surfaces and are not rapidly cleared from the hemolymph. The reason why *E. coli* bioparticles proved more valuable than live bacteria for the detection of cleaved CLIPA7 could be due to differences in their

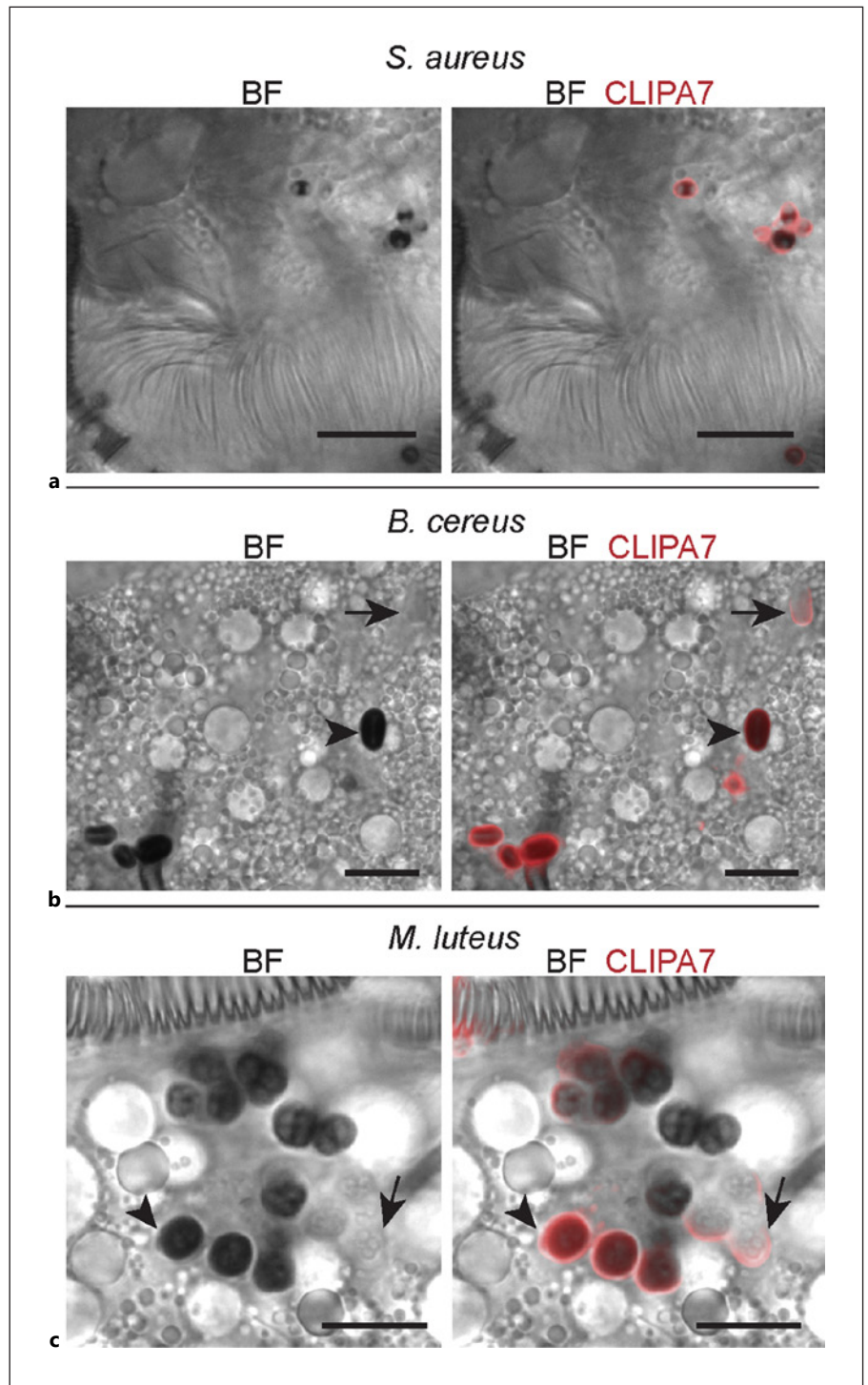


**Fig. 7.** CLIPA7 localizes to the surfaces of melanized and nonmelanized Gram-positive bacteria. Immunofluorescence assays showing CLIPA7 localization to nonfluorescent strains of *S. aureus* ( $OD_{600} = 2$ ) (a), *B. cereus* ( $OD_{600} = 2$ ) (b), and *M. luteus* ( $OD_{600} = 2$ ) (c) in dissected mosquito abdomens. Left panels correspond to bright field (BF) images and right panels to merged BF and red (CLIPA7) channel. Note CLIPA7 localization to surfaces of melanized (arrowheads) and nonmelanized (arrows) bacterial cells. Scale bars correspond to 10  $\mu\text{m}$ . All images were taken on a Leica upright fluorescence microscope and are representative of at least 2 independent biological experiments.

infection dynamics such as slower clearance of bioparticles, or in their surface biochemical characteristics that may trigger a more potent activation of immune responses or enhanced recruitment of immunity proteins to their surfaces.

*DsCLIPA7* mosquitoes exhibited consistently reduced endurance to *B. bassiana* infections, yet their resistance to the fungus was variable, in contrast to *dsTEP1* mosquitoes which showed a consistent reduction in resistance to *B. bassiana*. These results suggest that CLIPA7 plays a

secondary role in resistance to fungal infections which may be further nuanced by the hypomorphic phenotypes obtained with RNAi due to the incomplete depletion of proteins from the hemolymph. In support of this argument, CTL4 kd by RNAi has been always associated with a strong but incomplete melanization of *P. berghei* ookinetes [29, 49], whereas the depletion of CTL4 by CRISPR/Cas9 triggered the complete melanization of *P. berghei* ookinetes with no single live oocyst emerging in these mosquito midguts [61]. On the other hand, CLIPA7 is clearly involved in the clearance of *S. aureus* bacteria as its knockdown significantly enhanced their proliferation in mosquito tissues compared to control and even to *dsRel1* mosquitoes. To our knowledge, this is the first immunity gene in *A. gambiae* that exhibits a clear RNAi phenotype with respect to controlling *S. aureus* proliferation. In *A. gambiae*, anti-bacterial functions have been ascribed to several immunity genes including TEPI [36, 58], CTL4 [58, 62], Dscam [63], and several FBNs [64], however, in the context of controlling the proliferation of Gram-negative bacteria. Even mosquito Rel1 that occupies a key position in the Toll pathway, its knockdown does not always enhance *S. aureus* proliferation in our hands, as in this study, possibly because of its poor silencing efficiency [35, 65] or because the still poorly characterized Toll pathway in mosquitoes is not as efficient and essential as that in *Drosophila* [66, 67] in defense against Gram-positive bacteria. However, the fact that the survival of *dsRel1* mosquitoes to *S. aureus* infections was compromised suggests a role for the mosquito Toll pathway in enhancing host fitness in that context, possibly by promoting a wound healing response. Indeed, studies in *Drosophila* have provided increased evidence for the injury-induced activation of the Toll pathway [68, 69]. The increased *S. aureus* proliferation in *dsCLIPA7* mosquitoes did not compromise their survival, suggesting that *S. aureus* may be mildly pathogenic to mosquitoes which can well endure its presence in their tissues even at high levels. Mosquito lethality to *S. aureus* infections has been observed for several gene knockdowns in different studies [63, 70–72]; however, to our knowledge, in none of these knockdowns it was correlated with an increase in *S. aureus* proliferation.

CLIPA7 has a unique domain architecture among mosquito cSPHs, as it contains a long unstructured proline/glycine-rich region and an RGD motif in addition to the signature clip and protease-like domains; however, it is worth noting that an RGD motif is also present in CLIPA1, CLIPA5, CLIPA13, CLIPA14, and CLIPA26; hence, it is not unique to CLIPA7. These features together with

its association with bacterial surfaces suggest that it might tether bacteria to phagocytic receptors on hemocytes such as integrins. The fact that CLIPA7 labeled cells retained their cytosolic GFP suggests a role for this cSPH in bacterial clearance rather than lysis. The association of CLIPA7 with melanized Gram-positive bacteria may indicate a secondary role in the melanization of these bacteria since its knockdown did not reduce the melanotic excreta scored in MelASA in response to *S. aureus* and *M. luteus* infections. It may also indicate a role in the clearance of melanized cells from the hemolymph. Altogether, our results inform an essential role for CLIPA7 in the melanization of *E. coli* and in the clearance of *S. aureus* in a melanization-independent manner. The fact that CLIPA7 kd did not alter mosquito resistance nor endurance of *E. coli* infections indicates that melanization is not a primary defense response against *E. coli*, in agreement with previous studies from our laboratory [29, 31], which is not surprising owing to the primary roles of TEPI and CTL4 in this regard [36, 37, 58, 62]. The production of recombinant versions of CLIPA7 with deletions in the unstructured and RGD domains would be essential tools to study the relevance of these domains to CLIPA7 anti-bacterial function.

In conclusion, the structural features of CLIPA7 and its RNAi phenotypes clearly point to pleiotropic functions in mosquito immunity. Pleiotropy is a hallmark of immunity proteins observed at several levels and systems. Even antimicrobial peptides such as defensins that have simple structures have been assigned diverse roles in vertebrate immunity ranging from microbial membrane disruption [73, 74] to triggering chemotaxis [75, 76] and modulating inflammation [77]. It is difficult to perceive that the complex networks of CLIP genes, both cSPs and cSPHs, that regulate melanization have functions restricted within this narrow context. This is especially true for CLIPAs (cSPHs) and CLIPBs (cSPs), major components of these networks, which exhibit dynamic evolutionary profiles according to a recent study [78]. There has been an increased appreciation of the diverse functions attributed to certain components of the serine protease cascades regulating coagulation and complement in mammals [79–81]. Hence, it would not be surprising to observe that certain members of these CLIPs acquired additional functions along their evolutionary trajectory, equipping cSP cascades with diverse roles in insect immunity.

## Acknowledgments

We thank Kamal A. Shair, Central Research Laboratory, for providing free access to their equipment. We also thank Dr. Michael Povelones (University of Pennsylvania) for providing the CLIPC9 antibody and Dr. Zakaria Kambris (American University of Beirut) for providing the *Micrococcus luteus* strain.

## Statement of Ethics

This study was carried according to the recommendations in the Guide for the Care and Use of Laboratory Animals of the National Institutes of Health (Bethesda, USA). Animal protocol was approved by the Institutional Animal Care and Use Committee (IACUC) of the American University of Beirut (permit number 18-08-504). The IACUC functions in compliance with the Public Health Service Policy on the Humane Care and Use of Laboratory Animals (USA) and adopts the Guide for the Care and Use of Laboratory Animals of the National Institutes of Health.

## Conflict of Interest Statement

The authors have no conflicts of interest to declare.

## References

- 1 Cerenius L, Kawabata S, Lee BL, Nonaka M, Soderhall K. Proteolytic cascades and their involvement in invertebrate immunity. *Trends Biochem Sci.* 2010;35(10):575–83.
- 2 Kanost MR, Jiang H. Clip-domain serine proteases as immune factors in insect hemolymph. *Curr Opin Insect Sci.* 2015;11:47–55.
- 3 Nakhleh J, El Moussawi L, Osta MA. The melanization response in insect immunity. In: Ligoxygakis P, editor. *Insect immunity. advances in insect physiology.* Elsevier; 2017. Vol. 52; p. 2–20.
- 4 Veillard F, Troxler L, Reichhart JM. Drosophila melanogaster clip-domain serine proteases: structure, function and regulation. *Biochimie.* 2016;122:255–69.
- 5 Cao X, Gulati M, Jiang H. Serine protease-related proteins in the malaria mosquito, *Anopheles gambiae*. *Insect Biochem Mol Biol.* 2017;88:48–62.
- 6 Waterhouse RM, Kriventseva EV, Meister S, Xi Z, Alvarez KS, Bartholomay LC, et al. Evolutionary dynamics of immune-related genes and pathways in disease-vector mosquitoes. *Science.* 2007;316(5832):1738–43.
- 7 Cao X, He Y, Hu Y, Zhang X, Wang Y, Zou Z, et al. Sequence conservation, phylogenetic relationships, and expression profiles of non-digestive serine proteases and serine protease homologs in *Manduca sexta*. *Insect Biochem Mol Biol.* 2015;62:51–63.
- 8 Neafsey DE, Waterhouse RM, Abai MR, Aganezov SS, Alekseyev MA, Allen JE, et al. Mosquito genomics. Highly evolvable malaria vectors: the genomes of 16 *Anopheles* mosquitoes. *Science.* 2015;347(6217):1258522.
- 9 Zhao P, Wang GH, Dong ZM, Duan J, Xu PZ, Cheng TC, et al. Genome-wide identification and expression analysis of serine proteases and homologs in the silkworm *Bombyx mori*. *BMC Genomics.* 2010;11:405.
- 10 Kwon TH, Kim MS, Choi HW, Joo CH, Cho MY, Lee BL. A masquerade-like serine proteinase homologue is necessary for phenoloxidase activity in the coleopteran insect, *Holotrichia diomphalia* larvae. *Eur J Biochem.* 2000;267(20):6188–96.
- 11 Lee SY, Kwon TH, Hyun JH, Choi JS, Kawabata SI, Iwanaga S, et al. In vitro activation of pro-phenol-oxidase by two kinds of pro-phenol-oxidase-activating factors isolated from hemolymph of coleopteran, *Holotrichia diomphalia* larvae. *Eur J Biochem.* 1998;254(1):50–7.
- 12 Volz J, Muller HM, Zdanowicz A, Kafatos FC, Osta MA. A genetic module regulates the melanization response of *Anopheles* to *Plasmodium*. *Cell Microbiol.* 2006;8(9):1392–405.
- 13 Yu XQ, Jiang H, Wang Y, Kanost MR. Non-proteolytic serine proteinase homologs are involved in prophenoloxidase activation in the tobacco hornworm, *Manduca sexta*. *Insect Biochem Mol Biol.* 2003;33(2):197–208.
- 14 Kim MS, Baek MJ, Lee MH, Park JW, Lee SY, Soderhall K, et al. A new easter-type serine protease cleaves a masquerade-like protein during prophenoloxidase activation in *Holotrichia diomphalia* larvae. *J Biol Chem.* 2002;277(42):39999–40004.
- 15 Lee KY, Zhang R, Kim MS, Park JW, Park HY, Kawabata S, et al. A zymogen form of masquerade-like serine proteinase homologue is cleaved during pro-phenoloxidase activation by Ca<sup>2+</sup> in coleopteran and *Tenebrio molitor* larvae. *Eur J Biochem.* 2002;269(17):4375–83.
- 16 Jin Q, Wang Y, Hartson SD, Jiang H. Cleavage activation and functional comparison of *Manduca sexta* serine protease homologs SPH1a, SPH1b, SPH4, and SPH101 in conjunction with SPH2. *Insect Biochem Mol Biol.* 2022;144:103762.
- 17 Buchon N, Poidevin M, Kwon HM, Guillou A, Sottas V, Lee BL, et al. A single modular serine protease integrates signals from pattern-recognition receptors upstream of the Drosophila Toll pathway. *Proc Natl Acad Sci U S A.* 2009;106(30):12442–7.
- 18 Ji C, Wang Y, Guo X, Hartson S, Jiang H. A pattern recognition serine proteinase triggers the prophenoloxidase activation cascade in the tobacco hornworm, *Manduca sexta*. *J Biol Chem.* 2004;279(33):34101–6.

## Funding Sources

This work was supported by the National Institutes of Health, National Institute for Allergy and Infectious Disease, Grant R01 AI140760 (to M.A.O.), and by the University Research Board (Grant No. 104107) at the American University of Beirut. The funding sources had no role in the preparation of data or the manuscript.

## Author Contributions

Mike A. Osta conceived and designed the study and wrote the manuscript. Renée Zakhia performed all experimental work and critically reviewed and edited the manuscript. Mike A. Osta and Renée Zakhia analyzed the data.

## Data Availability Statement

All data generated or analyzed during this study are included in this article and its online supplementary material. Further inquiries can be directed to the corresponding author.

- 19 Roh KB, Kim CH, Lee H, Kwon HM, Park JW, Ryu JH, et al. Proteolytic cascade for the activation of the insect toll pathway induced by the fungal cell wall component. *J Biol Chem*. 2009;284(29):19474–81.
- 20 Takahashi D, Garcia BL, Kanost MR. Initiating protease with modular domains interacts with beta-glucan recognition protein to trigger innate immune response in insects. *Proc Natl Acad Sci U S A*. 2015;112(45):13856–61.
- 21 Wang Y, Jiang H. Interaction of beta-1, 3-glucan with its recognition protein activates hemolymph proteinase 14, an initiation enzyme of the prophenoloxidase activation system in *Manduca sexta*. *J Biol Chem*. 2006;281(14):9271–8.
- 22 Gupta S, Wang Y, Jiang H. *Manduca sexta* prophenoloxidase (proPO) activation requires proPO-activating proteinase (PAP) and serine proteinase homologs (SPHs) simultaneously. *Insect Biochem Mol Biol*. 2005;35(3):241–8.
- 23 Lu Z, Jiang H. Expression of *Manduca sexta* serine proteinase homolog precursors in insect cells and their proteolytic activation. *Insect Biochem Mol Biol*. 2008;38(1):89–98.
- 24 Kan H, Kim CH, Kwon HM, Park JW, Roh KB, Lee H, et al. Molecular control of phenoloxidase-induced melanin synthesis in an insect. *J Biol Chem*. 2008;283(37):25316–23.
- 25 Wang Q, Yin M, Yuan C, Liu X, Hu Z, Zou Z, et al. Identification of a conserved prophenoloxidase activation pathway in Cotton Bollworm *Helicoverpa armigera*. *Front Immunol*. 2020;11:785.
- 26 Gupta S, Wang Y, Jiang H. Purification and characterization of *Manduca sexta* prophenoloxidase-activating proteinase-1, an enzyme involved in insect immune responses. *Protein Expr Purif*. 2005;39(2):261–8.
- 27 Wang Y, Jiang H. Prophenoloxidase (proPO) activation in *Manduca sexta*: an analysis of molecular interactions among proPO, proPO-activating proteinase-3, and a cofactor. *Insect Biochem Mol Biol*. 2004;34(8):731–42.
- 28 Povelones M, Bhagavatula L, Yassine H, Tan LA, Upton LM, Osta MA, et al. The CLIP-domain serine protease homolog SPCLIP1 regulates complement recruitment to microbial surfaces in the malaria Mosquito *Anopheles gambiae*. *PLoS Pathog*. 2013;9(9):e1003623.
- 29 El Moussawi L, Nakhleh J, Kamareddine L, Osta MA. The mosquito melanization response requires hierarchical activation of non-catalytic clip domain serine protease homologs. *PLoS Pathog*. 2019;15(11):e1008194.
- 30 Nakhleh J, Christophides GK, Osta MA. The serine protease homolog CLIPA14 modulates the intensity of the immune response in the mosquito *Anopheles gambiae*. *J Biol Chem*. 2017;292(44):18217–26.
- 31 Schnitger AKD, Kafatos FC, Osta MA. The melanization reaction is not required for survival of *Anopheles gambiae* mosquitoes after bacterial infections. *J Biol Chem*. 2007;282(30):21884–8.
- 32 Yassine H, Kamareddine L, Chamat S, Christophides GK, Osta MA. A serine protease homolog negatively regulates TEP1 consumption in systemic infections of the malaria vector *Anopheles gambiae*. *J Innate Immun*. 2014;6(6):806–18.
- 33 Blandin S, Shiao SH, Moita LF, Janse CJ, Waters AP, Kafatos FC, et al. Complement-like protein TEP1 is a determinant of vectorial capacity in the malaria vector *Anopheles gambiae*. *Cell*. 2004;116(5):661–70.
- 34 Blandin SA, Wang-Sattler R, Lamacchia M, Gagneur J, Lycett G, Ning Y, et al. Dissecting the genetic basis of resistance to malaria parasites in *Anopheles gambiae*. *Science*. 2009;326(5949):147–50.
- 35 Kamareddine L, Nakhleh J, Osta MA. Functional interaction between apolipoporphins and complement regulate the mosquito immune response to systemic infections. *J Innate Immun*. 2016;8(3):314–26.
- 36 Levashina EA, Moita LF, Blandin S, Vriend G, Lagueux M, Kafatos FC. Conserved role of a complement-like protein in phagocytosis revealed by dsRNA knockout in cultured cells of the mosquito, *Anopheles gambiae*. *Cell*. 2001;104(5):709–18.
- 37 Moita LF, Wang-Sattler R, Michel K, Zimmermann T, Blandin S, Levashina EA, et al. In vivo identification of novel regulators and conserved pathways of phagocytosis in *A. gambiae*. *Immunity*. 2005;23(1):65–73.
- 38 Yassine H, Kamareddine L, Osta MA. The mosquito melanization response is implicated in defense against the entomopathogenic fungus *Beauveria bassiana*. *PLoS Pathog*. 2012;8(11):e1003029.
- 39 Sousa GL, Bishnoi R, Baxter RHG, Povelones M. The CLIP-domain serine protease CLIPC9 regulates melanization downstream of SP-CLIP1, CLIPA8, and CLIPA28 in the malaria vector *Anopheles gambiae*. *PLoS Pathog*. 2020;16(10):e1008985.
- 40 Franke-Fayard B, Trueman H, Ramesar J, Mendoza J, van der Keur M, van der Linden R, et al. A *Plasmodium berghei* reference line that constitutively expresses GFP at a high level throughout the complete life cycle. *Mol Biochem Parasitol*. 2004;137(1):23–33.
- 41 Blandin S, Moita LF, Kocher T, Wilm M, Kafatos FC, Levashina EA. Reverse genetics in the mosquito *Anopheles gambiae*: targeted disruption of the Defensin gene. *EMBO Rep*. 2002;3(9):852–6.
- 42 Garver LS, de Almeida Oliveira G, Barillas-Mury C. The JNK pathway is a key mediator of *Anopheles gambiae* antiplasmodial immunity. *PLoS Pathog*. 2013;9(9):e1003622.
- 43 Labrousse A, Chauvet S, Couillaud C, Kurz CL, Ewbank JJ. *Caenorhabditis elegans* is a model host for *Salmonella typhimurium*. *Curr Biol*. 2000;10(23):1543–5.
- 44 Malone CL, Boles BR, Lauderdale KJ, Thoenel M, Kavanaugh JS, Horswill AR. Fluorescent reporters for *Staphylococcus aureus*. *J Microbiol Methods*. 2009;77(3):251–60.
- 45 Kamareddine L, Fan Y, Osta MA, Keyhani NO. Expression of trypsin modulating oostatic factor (TMOF) in an entomopathogenic fungus increases its virulence towards *Anopheles gambiae* and reduces fecundity in the target mosquito. *Parasites Vectors*. 2013;6:22.
- 46 Muller HM, Dimopoulos G, Blass C, Kafatos FC. A hemocyte-like cell line established from the malaria vector *Anopheles gambiae* expresses six prophenoloxidase genes. *J Biol Chem*. 1999;274(17):11727–35.
- 47 Michel K, Suwanichinda C, Morlais I, Lambrechts L, Cohuet A, Awono-Ambene PH, et al. Increased melanizing activity in *Anopheles gambiae* does not affect development of *Plasmodium falciparum*. *Proc Natl Acad Sci U S A*. 2006;103(45):16858–63.
- 48 Mendes AM, Schlegelmilch T, Cohuet A, Awono-Ambene P, De Iorio M, Fontenille D, et al. Conserved mosquito/parasite interactions affect development of *Plasmodium falciparum* in Africa. *PLoS Pathog*. 2008;4(5):e1000069.
- 49 Osta MA, Christophides GK, Kafatos FC. Effects of mosquito genes on *Plasmodium* development. *Science*. 2004;303(5666):2030–2.
- 50 Christophides GK, Zdobnov E, Barillas-Mury C, Birney E, Blandin S, Blass C, et al. Immunity-related genes and gene families in *Anopheles gambiae*. *Science*. 2002;298(5591):159–65.
- 51 Kyte J, Doolittle RF. A simple method for displaying the hydropathic character of a protein. *J Mol Biol*. 1982;157(1):105–32.
- 52 Hayashi T, Nagai Y. The anomalous behavior of collagen peptides on sodium dodecyl sulfate-polyacrylamide gel electrophoresis is due to the low content of hydrophobic amino acid residues. *J Biochem*. 1980;87(3):803–8.
- 53 Michel K, Budd A, Pinto S, Gibson TJ, Kafatos FC. *Anopheles gambiae* SRPN2 facilitates midgut invasion by the malaria parasite *Plasmodium berghei*. *EMBO Rep*. 2005;6(9):891–7.
- 54 Bae YM, Jo YH, Patnaik BB, Kim BB, Park KB, Edosa TT, et al. *Tenebrio molitor* spatzle 1b is required to confer antibacterial defense against gram-negative bacteria by regulation of antimicrobial peptides. *Front Physiol*. 2021;12:758859.
- 55 Lemaitre B, Nicolas E, Michaut L, Reichhart JM, Hoffmann JA. The dorsoventral regulatory gene cassette spatzle/Toll/cactus controls the potent antifungal response in *Drosophila* adults. *Cell*. 1996;86(6):973–83.
- 56 Park S, Jo YH, Park KB, Ko HJ, Kim CE, Bae YM, et al. TmToll-7 plays a crucial role in innate immune responses against gram-negative bacteria by regulating 5 AMP genes in *Tenebrio molitor*. *Front Immunol*. 2019;10:310.
- 57 Shin SW, Bian G, Raikhel AS. A toll receptor and a cytokine, Toll5A and Spz1C, are involved in toll antifungal immune signaling in the mosquito *Aedes aegypti*. *J Biol Chem*. 2006;281(51):39388–95.

- 58 Dekmak AS, Yang X, Zu Dohna H, Buchon N, Osta MA. The route of infection influences the contribution of key immunity genes to antibacterial defense in *Anopheles gambiae*. *J Innate Immun*. 2021;13(2):107–26.
- 59 Zhang X, Li M, El Moussawi L, Saab SA, Zhang S, Osta MA, et al. CLIPB10 is a terminal protease in the regulatory network that controls melanization in the African malaria mosquito *Anopheles gambiae*. *Front Cell Infect Microbiol*. 2020;10:585986.
- 60 Zou Z, Shin SW, Alvarez KS, Kokoza V, Raikhel AS. Distinct melanization pathways in the mosquito *Aedes aegypti*. *Immunity*. 2010;32(1):41–53.
- 61 Simoes ML, Dong Y, Mlambo G, Dimopoulos G. C-type lectin 4 regulates broad-spectrum melanization-based refractoriness to malaria parasites. *PLoS Biol*. 2022;20(1):e3001515.
- 62 Schnitger AKD, Yassine H, Kafatos FC, Osta MA. Two C-type lectins cooperate to defend *Anopheles gambiae* against Gram-negative bacteria. *J Biol Chem*. 2009;284(26):17616–24.
- 63 Dong Y, Taylor HE, Dimopoulos G. AgDscam, a hypervariable immunoglobulin domain-containing receptor of the *Anopheles gambiae* innate immune system. *PLoS Biol*. 2006;4(7):e229.
- 64 Dong Y, Dimopoulos G. *Anopheles* fibrinogen-related proteins provide expanded pattern recognition capacity against bacteria and malaria parasites. *J Biol Chem*. 2009;284(15):9835–44.
- 65 Frolet C, Thoma M, Blandin S, Hoffmann JA, Levashina EA. Boosting NF- $\kappa$ B-dependent basal immunity of *Anopheles gambiae* aborts development of *Plasmodium berghei*. *Immunity*. 2006;25(4):677–85.
- 66 Gobert V, Gottar M, Matskevich AA, Rutschmann S, Royet J, Belvin M, et al. Dual activation of the *Drosophila* toll pathway by two pattern recognition receptors. *Science*. 2003;302(5653):2126–30.
- 67 Michel T, Reichhart JM, Hoffmann JA, Royet J. *Drosophila* Toll is activated by Gram-positive bacteria through a circulating peptidoglycan recognition protein. *Nature*. 2001;414(6865):756–9.
- 68 Capilla A, Karachentsev D, Patterson RA, Hermann A, Juarez MT, McGinnis W. Toll pathway is required for wound-induced expression of barrier repair genes in the *Drosophila* epidermis. *Proc Natl Acad Sci U S A*. 2017;114(13):E2682–8.
- 69 Evans CJ, Liu T, Girard JR, Banerjee U. Injury-induced inflammatory signaling and hematopoiesis in *Drosophila*. *Proc Natl Acad Sci U S A*. 2022;119(12):e2119109119.
- 70 Dong Y, Aguilar R, Xi Z, Warr E, Mongin E, Dimopoulos G. *Anopheles gambiae* immune responses to human and rodent *Plasmodium* parasite species. *PLoS Pathog*. 2006;2(6):e52.
- 71 Meister S, Agjanian B, Turlure F, Relogio A, Morlais I, Kafatos FC, et al. *Anopheles gambiae* PGRPLC-mediated defense against bacteria modulates infections with malaria parasites. *PLoS Pathog*. 2009;5(8):e1000542.
- 72 Meister S, Kanzok SM, Zheng XL, Luna C, Li TR, Hoa NT, et al. Immune signaling pathways regulating bacterial and malaria parasite infection of the mosquito *Anopheles gambiae*. *Proc Natl Acad Sci U S A*. 2005;102(32):11420–5.
- 73 Kagan BL, Selsted ME, Ganz T, Lehrer RI. Antimicrobial defensin peptides form voltage-dependent ion-permeable channels in planar lipid bilayer membranes. *Proc Natl Acad Sci U S A*. 1990;87(1):210–4.
- 74 Lehrer RI, Barton A, Daher KA, Harwig SS, Ganz T, Selsted ME. Interaction of human defensins with *Escherichia coli*. Mechanism of bactericidal activity. *J Clin Invest*. 1989;84(2):553–61.
- 75 Rohrl J, Yang D, Oppenheim JJ, Hehlhans T. Human beta-defensin 2 and 3 and their mouse orthologs induce chemotaxis through interaction with CCR2. *J Immunol*. 2010;184(12):6688–94.
- 76 Tjablinga GS, Ninaber DK, Drijfhout JW, Rabe KF, Hiemstra PS. Human cathelicidin LL-37 is a chemoattractant for eosinophils and neutrophils that acts via formyl-peptide receptors. *Int Arch Allergy Immunol*. 2006;140(2):103–12.
- 77 Semple F, Dorin JR. Beta-defensins: multifunctional modulators of infection, inflammation and more? *J Innate Immun*. 2012;4(4):337–48.
- 78 Ruzzante L, Feron R, Reijnders MJMF, Thiebaut A, Waterhouse RM. Functional constraints on insect immune system components govern their evolutionary trajectories. *Mol Biol Evol*. 2022;39(1):msab352.
- 79 Keragala CB, Draxler DF, McQuilten ZK, Medcalf RL. Haemostasis and innate immunity – a complementary relationship: a review of the intricate relationship between coagulation and complement pathways. *Br J Haematol*. 2018;180(6):782–98.
- 80 Megyeri M, Mako V, Beinrohr L, Doleschall Z, Prohaszka Z, Cervenak L, et al. Complement protease MASP-1 activates human endothelial cells: PAR4 activation is a link between complement and endothelial function. *J Immunol*. 2009;183(5):3409–16.
- 81 Renne T, Stavrou EX. Roles of factor XII in innate immunity. *Front Immunol*. 2019;10:2011.